Carbohydrate Polymers 118 (2015) 156–164

Contents lists available at ScienceDirect

Carbohydrate Polymers

journal homepage: www.elsevier.com/locate/carbpol

Complexation of estragole as pure compound and as main component of basil and tarragon essential oils with cyclodextrins

Miriana Kfoury[a,b], Lizette Auezova[a], Steven Ruellan[b], Hélène Greige-Gerges[a], Sophie Fourmentin[b,*]

[a] Bioactive Molecules Research Group, Doctoral School of Science and Technology, Department of Chemistry and Biochemistry, Faculty of Sciences-2, Lebanese University, Fanar, Lebanon
[b] Unité de Chimie Environnementale et Interactions sur le Vivant (UCEIV), ULCO, F-59140 Dunkerque, France

ARTICLE INFO

Article history:
Received 15 May 2014
Received in revised form 20 June 2014
Accepted 27 October 2014
Available online 20 November 2014

Keywords:
Estragole
Essential oils
Cyclodextrins
Formation constant
Photostability
DPPH• scavenging

ABSTRACT

Inclusion complexes of estragole (ES) as pure compound and as main component of basil and tarragon essential oils (EOs) with α-cyclodextrin (α-CD), β-cyclodextrin (β-CD), hydroxypropyl-β-cyclodextrin (HP-β-CD), randomly methylated-β-cyclodextrin (RAMEB), a low methylated-β-cyclodextrin (CRYSMEB) and γ-cyclodextrin (γ-CD) were characterized. Formation constants (K_f) of the complexes were determined in aqueous solution by nonlinear regression analysis using static headspace gas chromatography (SH-GC) and UV–visible spectroscopy. Solid inclusion complexes were prepared by the freeze-drying method for different CD:ES molar ratios and were characterized by differential scanning calorimetry (DSC) and Fourier transform infrared spectroscopy (FT-IR). Inclusion complexes formation allowed the controlled release of ES. Moreover, increased DPPH radical scavenging activity and photostability of ES and ES containing EOs (ESEOs) were observed in the presence of CDs. These findings suggest that encapsulation with CDs could be an efficient tool to improve the use of ES and ESEOs in aromatherapy, cosmetic and food fields.

1. Introduction

Estragole (1-methoxy-4-(2-propenyl)benzene, ES) is a natural constituent of a number of aromatic plants essential oils (EOs) such as basil, tarragon, anise, and fennel. ES naturally occurs in a variety of traditional foods, mainly in spices and is used as flavoring agent in seasonings, non-alcoholic beverages and condiments (Zeller, Horst, & Rychlik, 2009). Moreover, ES and ES containing EOs (ESEOs) can be used in food preservation due to their insecticidal, antiviral, antibacterial and acaricidal activities (Chang, Cho, & Li, 2009; Diao, Hu, Zhang, & Xu, 2014; Lee, 2005). The U.S. Department of Food and Agriculture listed ES and different ESEOs as generally recognized as safe (GRAS).

The use of ES as a natural food preservative and flavor is greatly limited by its volatility and low water solubility. Moreover, aromatic compounds can be sensitive to light and oxidation, resulting in an unwanted modification in taste, odor and color. To avoid these phenomena, compounds must be protected. Encapsulation is one of the options to preserve flavor in food products.

Nowadays, there has been a great interest in cyclodextrin (CD) encapsulation to increase the solubility and retention of poorly soluble substances. Encapsulation with CDs can improve the stability of sensitive ingredients (e.g. flavors, natural compounds), extend product shelf-life, protect it from oxidation and isomerization during storage and create a controlled release system of active substances (Ciobanu et al., 2012, 2013b; Pinho, Grootveld, Soares, & Henriques, 2014). Moreover, encapsulation allows EOs and their components to remain active as antimicrobial agents despite the harmful environmental conditions and long storage period (Marques, 2010).

CDs are non-toxic cyclic oligosaccharides consisted of (α-1,4)-linked α-D-glucopyrannose. They are obtained from enzymatic digestion of starch. CDs have a relatively hydrophilic external surface and a hydrophobic interior cavity (Szejtli, 1998). This conformation allows them to entrap hydrophobic molecules in their internal cavity forming non-covalent inclusion complexes, either in solution or solid state. An inclusion complex is a unique form of chemical structure in which guest molecule is enclosed within the cavity of the host. Most common native CDs are α-cyclodextrin (α-CD), β-cyclodextrin (β-CD) and γ-cyclodextrin (γ-CD) made up

* Corresponding author at: UCEIV, ULCO, 145, Avenue M. Schumann, 59140 Dunkerque, France.: Tel.: +33 03 28 65 82 54; fax: +33 03 28 23 76 05.
E-mail address: lamotte@univ-littoral.fr (S. Fourmentin).

http://dx.doi.org/10.1016/j.carbpol.2014.10.073
0144-8617/

of six, seven and eight glucosyl units, respectively. While the height of the cavity is the same for these native CDs, the number of glucose units determines the cavity diameter which in turn controls the size of the hydrophobic molecule that can be included. CD derivatives are also available on industrial scale and are widely used (Ciobanu et al., 2012; Ciobanu, Landy, & Fourmentin, 2013a).

This paper reports the first study of CD/ES inclusion complexes formation either in its pure form or in EOs, both in solution and in solid state. Static headspace-gas chromatography (SH-GC) and UV–visible were used to determine the stoichiometry and formation constants (K_f) of inclusion complexes in solution, while ^{1}H NMR was performed to evidence the inclusion of ES into the CD cavity. Solid inclusion complexes were prepared by the freeze-drying method at different molar ratios and characterized by differential scanning calorimetry (DSC) and Fourier transform infrared spectroscopy (FT-IR). Encapsulation efficiencies (EE%) and loading capacities were determined for the different molar ratios. Finally, the effects of CD encapsulation on DPPH scavenging activity, photostability and controlled release of guest molecules were explored.

2. Materials and methods

2.1. Materials

Estragole and 1,1-diphenyl-2-picrylhydrazyl (DPPH) were purchased from Aldrich. Methyl orange (MO) was purchased from Acros Organics. CRYSMEB (DS = 4.9) was provided from Roquette Frères (Lestrem, France), α-CD, β-CD, γ-CD, HP-β-CD (DS = 5.6) and RAMEB (DS = 12.6) were purchased from Wacker-Chemie (Lyon, France). All products were of analytical grade and were used as received. Basil essential oil (Ocimum basilicum var. basilicum, ES 64%, linalool, 26%) and tarragon essential oil (Artemisia dracunculus, ES 78%, β-ocimene, 17%) were purchased from Herbes et Traditions (Comines, France). Distilled deionized water was used all over the study.

2.2. Characterization of inclusion complexes in solution

The stoichiometry and formation constants (K_f) of the complexes were determined using static headspace gas chromatography (SH-GC) and UV–visible spectroscopy.

2.2.1. Static headspace gas chromatography (SH-GC)

K_f values for CD/ES were calculated using a SH-GC titration method developed in our laboratory for volatile organic compounds (Blach, Fourmentin, Landy, Cazier, & Surpateanu, 2008; Decock, Landy, Surpateanu, & Fourmentin, 2008). ES was added to 10 ml of water or CD solutions previously prepared and placed in 22 ml glass vials. Four CD concentrations (0.5, 4, 7, 10 mM) were used while ES concentration was kept constant (10 ppm). Vials were sealed using silicone septa and aluminium foil and thermostated at 25 ± 0.1 °C. After 24 h of equilibrium, 1 ml of vapor from the above solution was drawn out using a gas-tight syringe and injected in the chromatographic column via a transfer line. Measurements were done using an Agilent headspace autosampler and samples were analyzed by gas chromatography (Perkin Elmer Autosystem XL) equipped with a flame-ionization detector and an Agilent J&W DB-5 column. GC conditions were set as follows: detector temperature, 280 °C; column temperature, 160 °C; carrier gas, nitrogen.

In the case of ESEOs, 10 ppm of EO was added to 10 ml of water or 2 mM CD aqueous solutions. K_f values were calculated based on the ratio A_0/A of the peak area of ES in the absence and the presence of CD, A_0 and A, respectively, according to the following equation (Fourmentin, Ciobanu, Landy, & Wenz, 2013):

$$K_f = \frac{(A_0/A) - 1}{[CD]_0} \quad (1)$$

Temperature conditions were as follows: initial temperature of 50 °C for 2 min, increased to 190 °C at 5 °C/min giving a total run time of 30 min. All experiments were performed in triplicate.

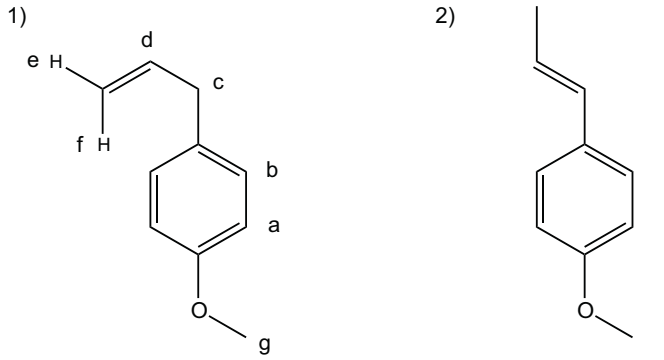

Fig. 1. Chemical structure of (1) estragole and (2) *trans*-anethole.

2.2.2. UV–visible measurements

This method is based on the spectral variation observed upon addition of guest (G) on a CD/methyl orange (MO) solution (Landy, Fourmentin, Salome, & Surpateanu, 2000).

2.2.2.1. Direct titration method. Before proceeding to the competition method, CD/MO inclusion complex was characterized by a direct titration method. For a 1:1 inclusion complex between CD and MO, K_f value was calculated as follows:

$$MO + CD \rightleftharpoons CD/MO \quad (2)$$

$$K_f = \frac{[CD/MO]}{[MO][CD]} \quad (3)$$

$$K_f \frac{[CD/MO]}{([MO]_T - [CD/MO])([CD]_T - [CD/MO])} \quad (4)$$

$$[CD/MO] = -\frac{1}{2}\sqrt{\left[\left(\frac{1}{K_f} + [CD]_T + [MO]_T\right)^2 - 4[CD]_T[MO]_T\right]} + \frac{1}{2}\left(\frac{1}{K_f} + [CD]_T + [MO]_T\right) \quad (5)$$

where K_f and T stand for formation constant and total, respectively. For each K_f value, the concentration of CD/MO inclusion complex is known and its spectral characteristic can be evaluated. An algorithmic treatment was applied to the first derivatives of UV spectra in order to avoid any spectral influence of diffraction phenomena (Landy et al., 2000).

2.2.2.2. Competition method. K_f values for CD/ES inclusion complexes were determined by a competition method designated as spectral displacement method. MO was used in its basic form. Two equilibria co-exist between CD, MO and ES and are expressed as follows:

$$MO + CD + ES \rightleftharpoons CD/MO + ES \rightleftharpoons CD/ES \quad (6)$$

Table 1
Formation constants (M^{-1}) values of CD/ES and CD/AN inclusion complexes obtained by UV–visible and SH-GC at 25 °C. Standard deviation values are < 10%.

Formation constants (M^{-1})	UV–visible	SH-GC			
	ES	ES	ES in basil	ES in tarragon	AN
α-CD	335	478	527	250	1163[a], 957[b]
β-CD	987	939	1140	1037	630[a], 441[b]
HP-β-CD	1508	1581	1318	1342	1042[a], 1083[b]
RAMEB	1916	1761	1903	1603	1553[a], 1209[b]
CRYSMEB	1584	1661	1622	1231	740[a], 759[b]
γ-CD	52	108	–	–	96[a]

[a] Ciobanu et al. (2013a).
[b] Kfoury et al. (2014).

An absorbance increment occurs after ES addition to the CD/MO solution. This increase allows the calculation of CD/ES K_f value. In fact, it is proportional to the replacement of MO molecules by ES inside the CD cavity. An algorithmic method was applied for data treatment. It took into consideration the two equilibria in an iterative way (Landy et al., 2000). All over the study, MO concentration was fixed at 0.1 mM and measurements were conducted between 520 and 530 nm. This wavelength range corresponds to the optimal spectral variation between the free and complexed forms of MO (Decock et al., 2006). All experiments were done in triplicate.

2.3. ^1H NMR spectroscopy

NMR experiments were recorded at 25 °C on a Bruker Avance III 400 spectrometer equipped with a BBFO probe. NMR measurements were carried out with standard Bruker pulses sequences. Samples were dissolved in 99.98% D_2O and filtered before use. One-dimensional spectra were run with FID resolution of 0.25 Hz/point, 4 s of acquisition time and 16 scans.

2.4. Preparation of solid inclusion complexes and physical mixtures

A freeze-drying method was used to prepare solid inclusion complexes in 1:1, 3:1 and 6:1 (CD:ES) molar ratios. Solutions were agitated for 24 h (300 rpm at 25 °C) and filtered through 0.45 μm filters to eliminate undissolved compounds. The filtrates were firstly frozen then lyophilized at −85 °C and 0 Pa in a Christ Alpha 2–4 LD Freeze dryer for approximately 48 h or until all moisture had been sublimated. The resulting powder was collected as CD/ES inclusion complex.

Physical mixtures (PM) were prepared by mixing the appropriate amounts of CD and ES in a mortar with a pestle.

Table 2
^1H chemical shift corresponding to β-CD and ES protons in the free and complexed state.

^1H assignment	δ (ppm)		Δδ* (ppm)
	β-CD free	Complex	
H-1	5.074	5.043	−0.031
H-2	3.651	3.623	−0.028
H-3	3.968	3.891	−0.077
H-4	3.587	3.564	−0.023
H-5	3.880	3.721	−0.159
H-6	3.880	3.834	−0.046
^1H assignment	δ (ppm)		Δδ* (ppm)
	ES free	Complex	
H-a	6.411	6.928	0.517
H-b	6.651	7.156	0.505
H-c	2.881	3.336	0.455
H-d	5.559	6.013	0.454
H-e	4.658	4.984	0.326
H-f	4.692	5.086	0.394
H-g	3.170	3.807	0.637

* A positive sign of Δδ ppm shows a downfield displacement and a negative sign an upfield displacement ($\Delta\delta = \delta_{complex} - \delta_{free}$).

2.5. Determination of encapsulation efficiency (EE%)

Amount of ES included in solid inclusion complexes was quantified spectrophotometrically. Ten miligrams of each CD/ES solid inclusion complex were dissolved in 10 ml ethanol. This treatment leads to the release of encapsulated ES. Subsequently, UV–visible absorbance measurements were conducted after appropriate dilution of samples. All preparations and experiments were done in triplicate.

Encapsulation efficiency (EE%) values were calculated as follows:

$$EE\% = \frac{ES_{exp}\,(mg)}{ES_t\,(mg)} \times 100 \quad (7)$$

where ES_{exp} is the calculated ES amount in the freeze dried inclusion complex (determined experimentally) and ES_t stands for the theoretical ES amount initially used to prepare the solid inclusion complex. The loading capacities of CDs were also expressed as mg of encapsulated ES per gram of solid inclusion complexes.

2.6. Differential scanning calorimetry (DSC)

DSC measurements were conducted for ES, CDs, their solid inclusion complexes and physical mixtures by a Mettler-Toledo DSC821 differential calorimeter (Mettler-Toledo S.P.A., Milan, Italy). Indium was used for calibration. Accurately weighted amounts (3–5 mg) of samples were placed in perforated aluminum pans and heated (scanning rate: 10 °C/min, scanning range: 50 to 300 °C, nitrogen purge gas flow rate: 40 ml/min). An empty pan sealed in the same way was used as reference. Reproducibility was checked out by running the sample in triplicate.

2.7. Fourier transform infrared spectroscopy (FT-IR)

FT-IR spectra were recorded in the region of 400–4000 cm^{-1} for free ES, CDs and inclusion complexes using a Fourier Transform Infrared spectrometer (FT/IR-6300, JASCO, Japan). FTIR samples were prepared in the form of potassium bromide pellets.

2.8. DPPH radical scavenging method

The 1,1-diphenyl-2-picryl-hydrazil (DPPH•) radical scavenging activity of ES, ESEOs and their inclusion complexes was measured using the method described by Brand-Williams, Cuvelier, and Berset (1995) with some modifications. An ethanolic solution

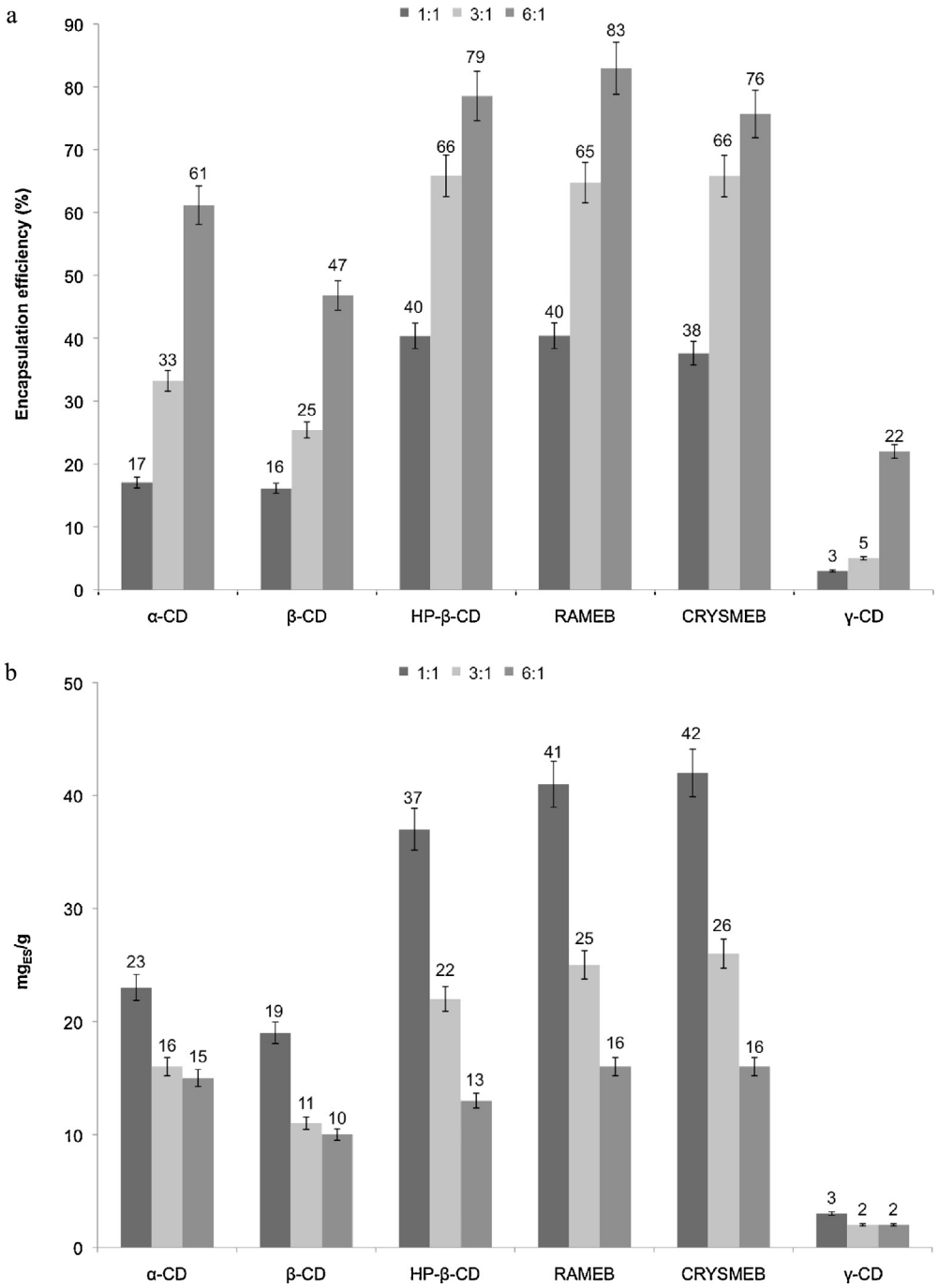

Fig. 2. (a) Encapsulation efficiency (EE%) values and (b) loading capacity (mg of encapsulated ES per gram of complex powder) for different CD:ES molar ratios. Standard deviation values are <10%.

of DPPH• (0.1 mM) was prepared. Then, 2 ml of this solution were added to 2 ml of sample solutions (20 ppm of ES or ESEOs alone or in the presence of 10 mM CDs). Mixtures were shaken 15 h and allowed to stand at 25 °C in the dark. The absorbance was measured at 520 nm. Blank sample was prepared by mixing 2 ml of distilled water with 2 ml of DPPH• solution. All preparations and assays were performed in triplicate. Results were expressed as percentage of DPPH• elimination calculated as follows:

$$AU\% = \left(1 - \frac{A_S}{A_0}\right) \times 100 \quad (8)$$

where AU% stands for radical scavenging activity, A_s is the absorbance of sample (ES, ESEOs or complexes) and A_0 is the absorbance of blank sample.

2.9. Photostability studies

Photostability studies were performed in solution and in solid state using a Multirays apparatus (Heliosquartz) equipped with 10 UVC lamps (254 nm, 15 W each). In the case of aqueous solution experiments, ES (40 ppm) or ESEOs (40 ppm) were added to water or CD solution (10 mM), agitated as described above (Section 2), then filtered through 0.45 μm filters. Filtrates were then transferred in a quartz reactor and exposed to UVC irradiation. Solid state experiments were carried out by spreading inclusion complexes or physical mixtures on watch glass prior to irradiation. The physical mixture of ES with glucose was used as reference. At each time interval, 0.5 ml of solutions or 10 mg of solid inclusion complexes and physical mixtures were withdrawn

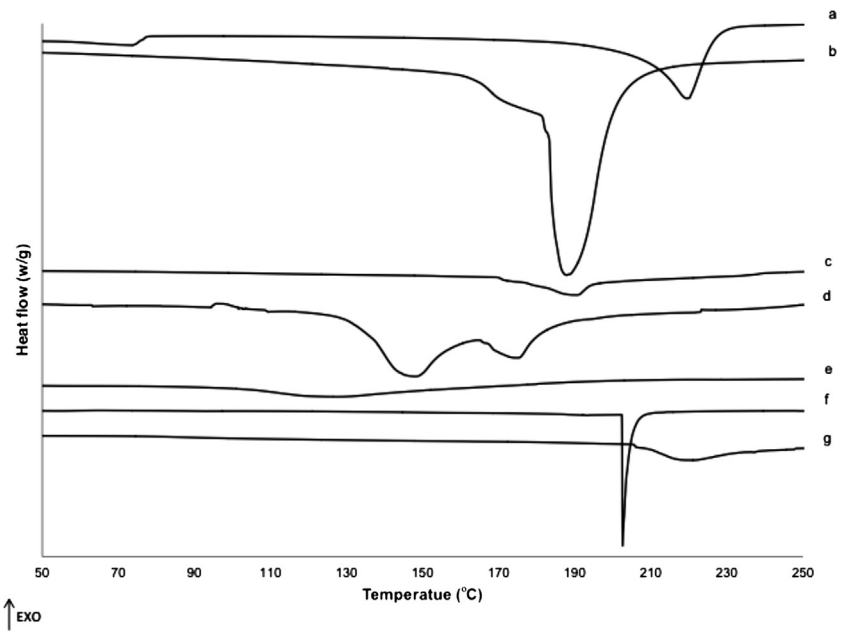

Fig. 3. DSC thermograms of (a) ES, (b) β-CD, (c) β-CD/ES inclusion complex, (d) β-CD/ES physical mixture, (e) HP-β-CD, (f) HP-β-CD/ES inclusion complex and (g) HP-β-CD/ES physical mixture.

and diluted or dissolved in water, respectively. The concentration of ES was determined by SH-GC. Experiments were performed twice.

Results were expressed as percentages of remaining ES using the following equation:

$$\text{Remaining ES\%} = \frac{C_t}{C_0} \times 100 \quad (9)$$

where C_0 is the initial concentration of ES in the samples and C_t the concentration at time t.

2.10. Controlled release studies

Solutions were prepared as described for photostability experiments, sprayed evenly on filter papers placed in a 22 mL glass vial, and allowed to volatilize at room temperature. At different time intervals, vials were sealed and residual ES on the filter was determined by SH-GC (Yuan, Lu, & Jin, 2014). Experiments were repeated twice.

3. Results and discussion

3.1. Determination of formation constants (K_f)

3.1.1. Static headspace gas chromatography (SH-GC)

K_f values (Table 1) were obtained using an algorithmic treatment for ES as pure compound or in EOs using Eq. (1) (Fourmentin et al., 2013; Landy et al., 2000). To the best of our knowledge, no data were reported previously for CD/ES inclusion complexes. For all the studied CDs, the experimental variations of the peak area of ES fit well with the theoretical curve for a 1:1 inclusion complex in agreement with a 1:1 stoichiometry.

It could be noticed that, among the studied CDs, β-CD and its derivatives showed the highest K_f values with β-CD derivatives showing higher affinity for ES than native β-CD. K_f values for ES and ESEOs were in the same order of magnitude. Consequently, further studies could use ES as a model for ESEOs.

We compared K_f values obtained for ES to those obtained for *trans*-anethole (AN) (Ciobanu et al., 2013a; Kfoury, Auezova, Greige-Gerges, Ruellan, & Fourmentin, 2014). AN and ES differ only by the position of the double bond in the propenyl side chain (Fig. 1).

The main difference in the K_f values was noted for α-CD. This could be explained by the restriction of the rotation of the double bond when located in the middle of the propenyl chain of AN, resulting in a planar, linear and rigid structure of AN which fits more with the small cavity of α-CD than ES. In the opposite, in ES the double bond can undergo free rotation around the carbon-carbon single bond increasing the steric hindrance.

In the same way as AN, K_f values of CD/ES are adequate to allow a controlled release of ES and improve its bioavailability since they fall in the range 200–10,000 M^{-1} (Aicart & Junquera, 2003; Vandelli et al., 2000).

3.1.2. UV–visible analysis

A UV–visible competition method was also applied to calculate K_f values for CD/ES inclusion complexes. Such a method is based on the spectral variation observed upon addition of guest on a CD/MO solution (Decock et al., 2006).

In a first step, K_f values of CD/MO complexes were calculated by a direct titration method. K_f values were found to be in good agreement with those from literature (Decock et al., 2006).

Upon ES addition, an increase in MO absorbance was observed indicating the formation of CD/ES inclusion complexes. These spectral variations were in agreement with a 1:1 host/guest stoichiometry. K_f values (Table 1) were calculated using an algorithmic procedure and were consistent with data obtained by SH-GC.

3.2. ^{1}H NMR spectroscopy

To prove the inclusion of ES inside the CD cavity, ^{1}H NMR spectroscopy studies of free ES, free β-CD and β-CD/ES inclusion complex were undertaken. Indeed, after inclusion complex formation, the H-3 and H-5 atoms, located inside the CD cavity will be considerably shielded while the external surface hydrogens H-1, H-2 and H-4 will show no or marginal shifts (Singh, Bharti, Madan, & Hiremath, 2010). Moreover, hydrogen atoms of the guest will be also shielded when inclusion occurs. The ^{1}H chemical shifts of β-CD and ES in the free and complexed state are summarized in Table 2.

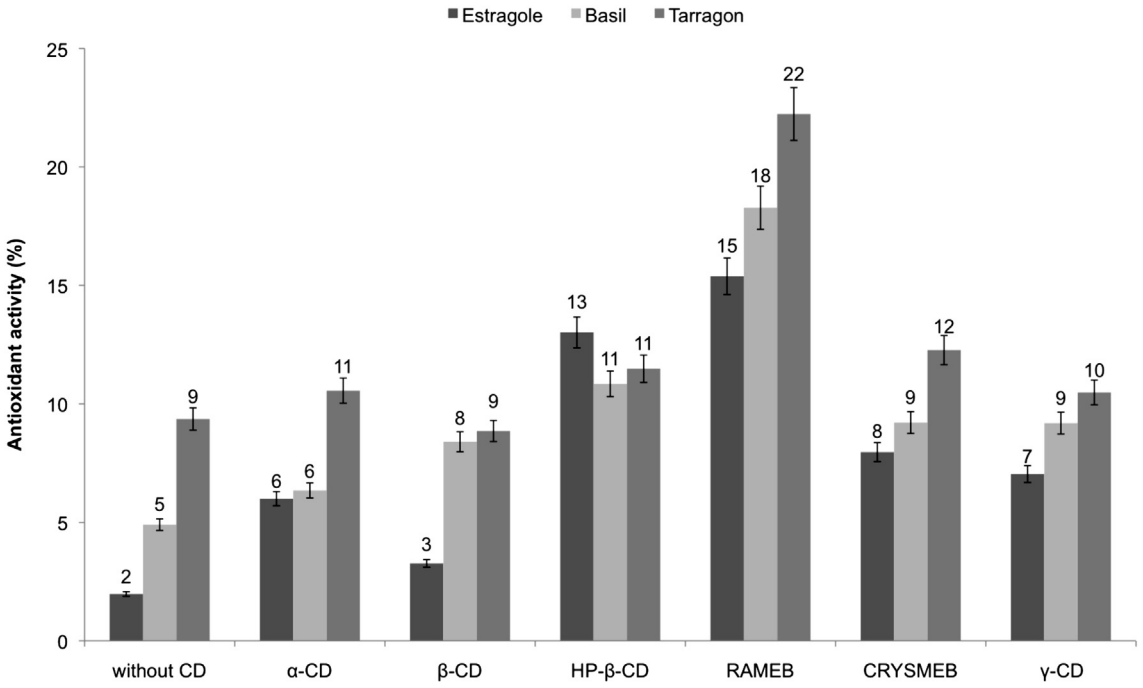

Fig. 4. DPPH• radical scavenging activity of ES, ESEOs and their inclusion complexes with the studied CDs. Standard deviation values are <5%.

As expected, the largest upfield shifts were observed for the H-3 and H-5 hydrogens, which are located inside the CD cavity. The H-6 also experienced a considerable upfield shift while H-1, H-2 and H-4 were less affected. These proved that interactions occur between ES and the CD cavity during complexation. The upfield shift of H-3 and H-5 protons of the β-CD cavity indicated that H-3 and H-5 protons are located near to a π-electron cloud which induced a magnetic anisotropic shielding. This suggested that the benzene ring of ES is embedded inside the CD cavity (Fernandes, Carvalho, da Costa, & Veiga, 2003). Furthermore, all ES hydrogens suffered downfield shifts due to the modification in the polarity of their surrounding environment when they are included inside the cavity (Djedaini, Lin, Perly, & Wouessidjewe, 1990).

3.3. Determination of ES in solid inclusion complexes

Solid inclusion complexes were prepared for different CD:ES molar ratios using the freeze-drying method. Freeze-drying is especially used for volatile and thermolabile molecules, because the low temperature minimizes their losses (Del Valle, 2004).

The amount of ES included in the solid complexes was measured by UV–visible spectroscopy and results were expressed as encapsulation efficiency (EE%) and loading capacity (mg of encapsulated ES per gram of complex powder) (Fig. 2).

The encapsulation efficiency (EE%) increased by increasing the CD proportion reaching over 60% or 80% of encapsulation in the RAMEB/ES system at 3:1 and 6:1 molar ratios respectively. This increase of EE% with molar ratio is coherent with data from literature (Dos Santos, Buera, Mazzobre, 2012). Our results showed relatively low EE% as compared with data for other essential oil components (Seo, Min, & Choi, 2010) but are in agreement with those for *trans*-anethole (Kfoury et al., 2014). This low EE% could be attributed to the very low aqueous solubility of ES. Whatever the molar ratio used, the highest EE% values were observed for β-CD derivatives (Fig. 2a). These results were in good correlation with corresponding K_f values (Table 1), except for β-CD.

On the opposite, the amount of ES encapsulated per gram of solid inclusion complex powder decreases with the increase in the initial proportion of CD (Fig. 2b). At all molar ratios, β-CD derivatives showed the highest loading capacities. For toxicological and cost considerations, formulation bulk and drug bioavailability, it is desirable to minimize as much as possible the amount of CD, especially, in pharmaceutical formulations (Loftsson, Hreinsdottir, & Masson, 2005; Rao & Stella, 2003). Therefore, only the inclusion complexes prepared with 1:1 molar ratio will be further investigated.

3.4. Differential scanning calorimetry analyses

Fig. 3 depicts the DSC thermograms of ES, β-CD, HP-β-CD, their inclusion complexes and physical mixtures. The thermogram of pure ES exhibited an endothermic peak at 220 °C (Fig. 3a) corresponding to its boiling point.

β-CD and HP-β-CD (Fig. 3b and e) curves showed one wide endothermic event each corresponding to the melting point of β-CD (at about 186 °C) and the release of water molecules from HP-β-CD cavity (between 100 and 150 °C). The endothermic peak of ES had disappeared in the thermograms of β-CD/ES and HP-β-CD/ES inclusion complexes (Fig. 3c and f). In fact, disappearance of thermal peaks of the guest molecule is generally considered as an evidence of its encapsulation in the CD (Nieddu et al., 2014).

DSC patterns of the physical mixtures (Fig. 3d and g) showed the presence of both pure compounds peaks with slight shifts indicating that there was no homogeneous structure and that no inclusion took place when CDs and ES were simply mixed together. Our observations were consistent with those found in the literature (Hu, Zhang, Song, Gu, & Hu, 2012; Wang, Luo, & Xiao, 2014).

3.5. Fourier transform infrared spectroscopy analyses

The encapsulation of ES did not cause significant alterations of the FT-IR bands of free CDs indicating that no strong interaction existed between ES and C—C, C—O—C or OH groups of CDs (data not shown). Upon encapsulation, ES bands at 3084, 3042, 1612, 1516, 1464, 994 and 812 cm^{-1} were not observed anymore in the complexes spectra. Nevertheless, some peaks of ES (at 1262

and 846 cm^{-1} attributed, respectively, to υ(C—O—C) and δ(C—H) of *p*-substituted benzene) are still detected in the spectra of inclusion complexes. However, they represented a very low strength probably due the low ES quantity (10–15% w/w) in the inclusion complexes as compared to the massive host. This could be also due to the restriction of ES inside the CD cavity (Yang & Song, 2005). In addition, the O—H stretching band at 3402 cm^{-1} in β-CD/ES and at 3424 cm^{-1} in HP-β-CD/ES were found to be shifted to lower frequencies as compared to those of β-CD and HP-β-CD, respectively. These changes may be associated with a reorganization of the intramolecular hydrogen bonds due to the formation of intermolecular hydrogen bonds between ES and CDs within the inclusion complexes and/or to the change in degree of hydration.

These results indicated that ES was successfully included in the hydrophobic cavity of CDs.

3.6. Determination of DPPH radical scavenging activity

DPPH• can accept an electron or hydrogen radical to form a stable molecule. It is usually used to evaluate the antioxidant activity. It is well known that antioxidant activity of phenolic compounds depends on the position of the hydroxyl group and on the degree of hydroxylation, as well as the nature of the substituents on the aromatic cycle (Brand-Williams et al., 1995). Furthermore, the DPPH• radical scavenging ability of an antioxidant is believed to be closely associated with its hydrogen-donating ability.

ES alone showed a very poor radical scavenging activity (Fig. 4). This result is in good agreement with literature (Lee, Umano, Shibamoto, & Lee, 2005). This could be attributed to the fact that ES carries no hydrogen atom donor. In addition, the double bond of its propenyl moiety is not conjugated with the aromatic ring that inhibits the formation of a conjugated radical cation (Brand-Williams et al., 1995). The better antioxidant activity of ESEOs (Fig. 4) may be ascribed to the synergistic effects of their diverse major and minor components (Liang, Yuan, Vriesekoop, & Lv, 2012) such as β-ocimene, in tarragon EO and linalool in basil EO.

A notable scavenging activity was generally observed with all CDs for ES and ESEOs (Fig. 4). This could be explained by the formation of hydrogen bonds between CDs and ES as well as between CDs and other ESEOs components improving the hydrogen-donating ability of guest molecules (Shao, Zhang, Fang & Sun, 2014). No significant decrease in the absorbance of DPPH• solution was observed in presence of CDs alone implying that CDs have no radical scavenging activity themselves.

3.7. Photostability studies

It is known that photodegradation of compounds could be hindered through host/guest inclusion complex formation (Hu et al., 2012). In the present work, the photostability of ES, ESEOs, and their inclusion complexes was examined in aqueous solution and in solid state under UVC stress. Results are illustrated in Fig. 5. We can obviously note that for all the samples, ES degradation followed a first-order kinetic rate. Fig. 5a shows the degradation of ES and its inclusion complexes in aqueous solution. ES was completely degraded after 40 min of UVC exposure. We could notice that degradation of ES was slowed down when included in CDs except for γ-CD. This could be explained by the fact that γ-CD/ES has a very low K_f value. Thus, it is evident that the protecting effect of CDs was due to the inclusion of ES in the cavity of CDs.

After an hour of irradiation, between 32 and 70% of ES was still remaining in solution in the presence of CDs (except for γ-CD). The calculated degradation rate constants were 0.1092, 0.091, 0.0176, 0.0117, 0.0061, 0.013 and 0.1025 for ES, α-CD, β-CD, HP-β-CD, RAMEB, CRYSMEB and γ-CD respectively under UVC irradiation.

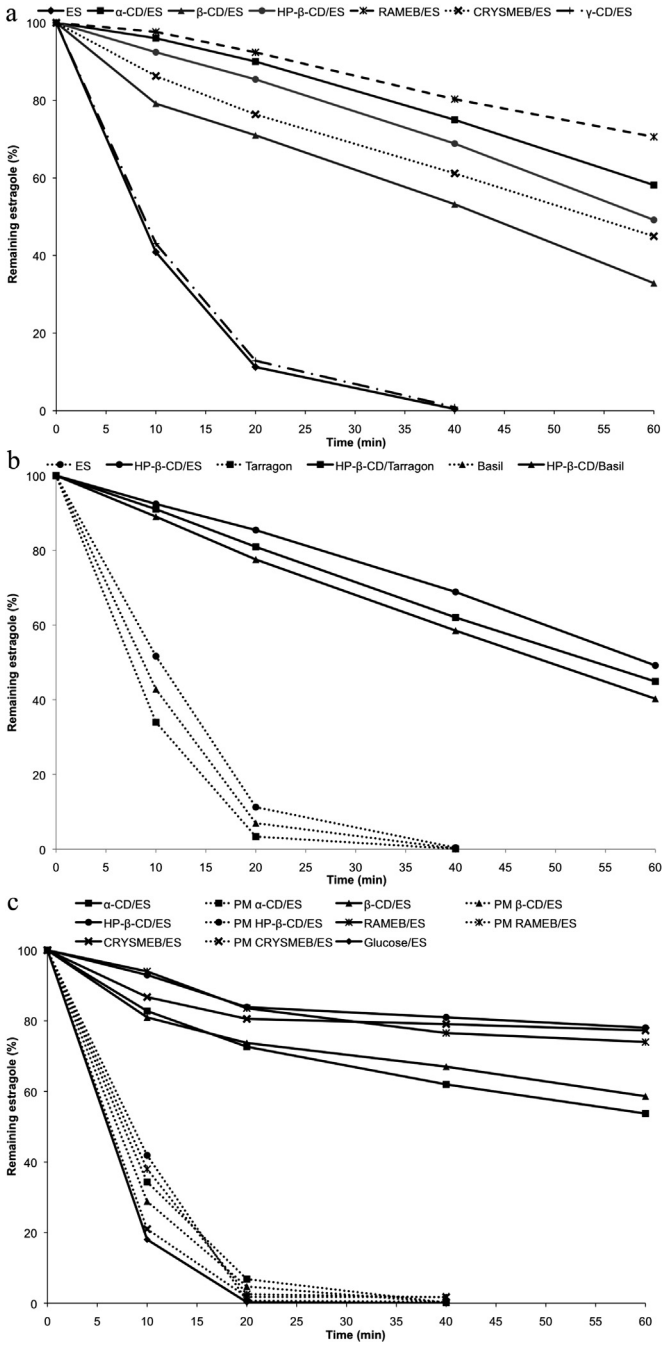

Fig. 5. Photodegradation profiles of (a) ES in water and in CD solutions, (b) ESEOs in water and in HP-β-CD solution and (c) solid inclusion complexes and physical mixtures under UVC irradiation.

Moreover, HP-β-CD was chosen to investigate the influence of the complexation on the photodegradation of ES in basil and tarragon EOs (Fig. 5b). We could notice that ES degradation is more pronounced in both ESEOs as compared to pure ES. Indeed, in complex mixtures like EOs, alterations taking place in a compound may also influence stability of other molecules (Turek & Stintzing, 2013). However, ESEOs encapsulation with HP-β-CD showed an improvement in ES stability comparable with that of pure ES. These observations proved that CD also exerts a protective effect on ES stability in EOs mixtures.

To our knowledge, this is the first study on the photodegradation of solid CD inclusion complexes. Fig. 5c clearly shows the protective effect of inclusion complexes as compared to physical mixtures.

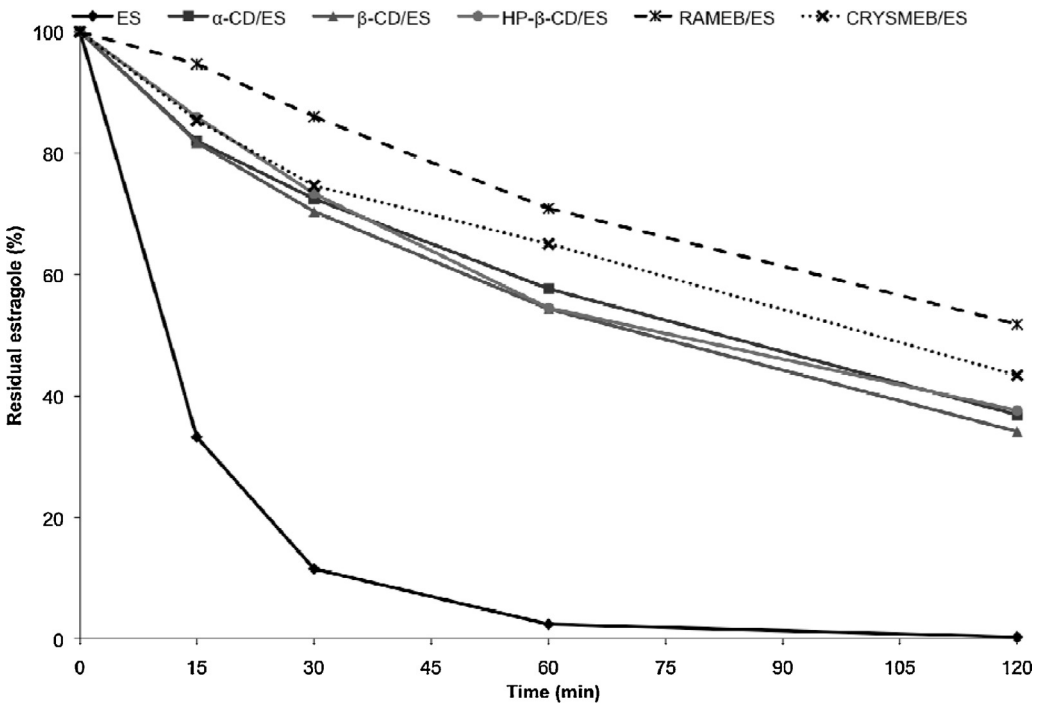

Fig. 6. Residual rate of ES and CD/ES inclusion complexes.

Degradation of ES in its pure form (mixed to glucose) and in the physical mixtures was similar. ES was completely disappeared after 40 min of irradiation whereas 54–78% of ES was still remaining in the solid complexes after 1 h of irradiation. Inclusion complexes slowed down the photodegradation of ES by 14, 19, 23, 26 and 19 times for α-CD, β-CD, HP-β-CD, RAMEB and CRYSMEB, respectively, as compared to the corresponding physical mixtures. These results indicated an important improvement of the photostability of ES upon CD encapsulation in solid state.

3.8. Controlled release studies

Release profiles of ES and its inclusion complexes are illustrated in Fig. 6. We could notice that, all over the study, the percentage of residual ES in all inclusion complexes was considerably higher than that of free ES. Furthermore, free ES level showed a rapid decrease (98% in 1 h) while inclusion complexes showed steadier profiles and sustained release of ES. After 2 h, residual ES was 37, 34, 38, 52, and 44% for α-CD, β-CD, HP-β-CD, RAMEB, and CRYSMEB inclusion complexes, respectively (Fig. 6). The results clearly demonstrated that encapsulation in CDs allowed the controlled release of ES. Our findings were in good agreement with previous reports for CD/EOs inclusion complexes (Ciobanu et al., 2012, 2013b; Yuan et al., 2014).

4. Conclusion

This study clearly demonstrated that α-CD, β-CD, HP-β-CD, RAMEB and CRYSMEB can form stable inclusion complexes with ES and ESEOs. Therefore, CDs can be used for the encapsulation/release of this flavor compound. Formation constants (K_f) determined via SH-GC and UV–visible, were in good agreement. DSC and FT-IR confirmed the formation of inclusion complexes in the solid form. Photostability of ES and ESEOs was significantly enhanced by CD encapsulation. Moreover, antioxidant activity of ES and ESEOs was increased by the formation of inclusion complexes with CDs. Finally, the formation of inclusion complexes allowed a controlled release of ES. These findings suggested that the complexation with CDs could be an effective way to improve the stability and antioxidant activity of ES and ESEOs as well as to sustain the guest release.

Acknowledgments

Authors would like to thank Benoit Duponchel for DSC analyses. Authors are grateful to Lebanese National Council for Scientific Research (CNRS-L) for the financial support of M. Kfoury's PhD thesis. The study was financially supported by the Doctoral School of Science and Technology of Lebanese University (ER28). UCEIV participates in the Institut de Recherche en ENvironnement Industriel (IRENI) financed by the Communauté Urbaine de Dunkerque, the Région Nord Pas-de-Calais, the Ministère de l'Enseignement Supérieur et de la Recherche, the CNRS and European Regional Development Fund (ERDF).

References

Aicart, E., & Junquera, E. (2003). Complex formation between purine derivatives and cyclodextrins: A fluorescence spectroscopy study. *Journal of Inclusion Phenomena and Macrocyclic Chemistry*, *47*(3–4), 161–165.

Blach, P., Fourmentin, S., Landy, D., Cazier, F., & Surpateanu, G. (2008). Cyclodextrins: A new efficient absorbent to treat waste gas streams. *Chemosphere*, *70*(3), 374–380.

Brand-Williams, W., Cuvelier, M. E., & Berset, C. (1995). Use of a free radical method to evaluate antioxidant activity. *LWT—Food Science and Technology*, *28*(1), 25–30.

Chang, C., Cho, L. K., & Li, Q. X. (2009). Insecticidal activity of basil oil, *trans*-anethole, estragole, and linalool to adult fruit flies of *Ceratitis capitata*, *Bactrocera dorsalis*, and *Bactrocera cucurbitae*. *Journal of Economic Entomology*, *102*(1), 203–209.

Ciobanu, A., Landy, D., & Fourmentin, S. (2013a). Complexation efficiency of cyclodextrins for volatile flavor compounds. *Food Research International*, *53*(1), 110–114.

Ciobanu, A., Mallard, I., Landy, D., Brabie, G., Nistor, D., & Fourmentin, S. (2012). Inclusion interactions of cyclodextrins and crosslinked cyclodextrin polymers with linalool and camphor in *Lavandula angustifolia* essential oil. *Carbohydrate Polymers*, *87*(3), 1963–1970.

Ciobanu, A., Mallard, I., Landy, D., Brabie, G., Nistor, D., & Fourmentin, S. (2013b). Retention of aroma compounds from *Mentha piperita* essential oil by cyclodextrins and crosslinked cyclodextrin polymers. *Food Chemistry*, *138*(1), 291–297.

Decock, G., Fourmentin, S., Surpateanu, G. G., Landy, D., Decock, P., & Surpateanu, G. (2006). Experimental and theoretical study on the inclusion compounds of aroma components with β-cyclodextrins. *Supramolecular Chemistry*, *18*(6), 477–482.

Decock, G., Landy, D., Surpateanu, G., & Fourmentin, S. (2008). Study of the retention of aroma components by cyclodextrins by static headspace gas chromatography. *Journal of Inclusion Phenomena and Macrocyclic Chemistry*, *62*(3–4), 297–302.

Del Valle, E. M. M. (2004). Cyclodextrins and their uses: A review. *Process Biochemistry*, *39*(9), 1033–1046.

Diao, W. R., Hu, Q. P., Zhang, H., & Xu, J. G. (2014). Chemical composition, antibacterial activity and mechanism of action of essential oil from seeds of fennel (*Foeniculum vulgare* Mill.). *Food Control*, *35*(1), 109–116.

Djedaini, F., Lin, S. Z., Perly, B., & Wouessidjewe, D. (1990). High-field nuclear magnetic resonance techniques for the investigation of a β-cyclodextrin: indomethacin inclusion complex. *Journal of Pharmaceutical Sciences*, *79*(7), 643–646.

Dos Santos, C., Buera, M. P., & Mazzobre, M. F. (2012). Influence of ligand structure and water interactions on the physical properties of β-cyclodextrins complexes. *Food Chemistry*, *132*(4), 2030–2036.

Fernandes, C. M., Carvalho, R. A., da Costa, S. P., & Veiga, F. G. B. (2003). Multimodal molecular encapsulation of nicardipine hydrochloride by β-cyclodextrin, hydroxypropyl-β-cyclodextrin and triacetyl-β-cyclodextrin in solution. Structural studies by ^{1}H NMR and ROESY experiments. *European Journal of Pharmaceutical Sciences*, *18*(5), 285–296.

Fourmentin, S., Ciobanu, A., Landy, D., & Wenz, G. (2013). Space filling of β-cyclodextrin and β-cyclodextrin derivatives by volatile hydrophobic guests. *Beilstein Journal of Organic Chemistry*, *9*, 1185–1191.

Hu, L., Zhang, H., Song, W., Gu, D., & Hu, Q. (2012). Investigation of inclusion complex of cilnidipine with hydroxypropyl-β-cyclodextrin. *Carbohydrate Polymers*, *90*(4), 1719–1724.

Kfoury, M., Auezova, L., Greige-Gerges, H., Ruellan, S., & Fourmentin, S. (2014). Cyclodextrin, an efficient tool for *trans*-anethole encapsulation: Chromatographic, spectroscopic, thermal and structural studies. *Food Chemistry*, *164*, 454–461.

Landy, D., Fourmentin, S., Salome, M., & Surpateanu, G. (2000). Analytical improvement in measuring formation constants of inclusion complexes between β-cyclodextrin and phenolic compounds. *Journal of Inclusion Phenomena and Macrocyclic Chemistry*, *38*(1–4), 187–198.

Lee, H. S. (2005). Food protective effect of acaricidal components isolated from anise seeds against the stored food mite, *Tyrophagus putrescentiae* (Schrank). *Journal of Food Protection*, *68*(6), 1208–1210.

Lee, S. J., Umano, K., Shibamoto, T., & Lee, K. G. (2005). Identification of volatile components in basil (*Ocimum basilicum* L.) and thyme leaves (*Thymus vulgaris* L.) and their antioxidant properties. *Food Chemistry*, *91*(1), 131–137.

Liang, H., Yuan, Q., Vriesekoop, F., & Lv, F. (2012). Effects of cyclodextrins on the antimicrobial activity of plant-derived essential oil compounds. *Food Chemistry*, *135*(3), 1020–1027.

Loftsson, T., Hreinsdottir, D., & Masson, M. (2005). Evaluation of cyclodextrin solubilization of drugs. *International Journal of Pharmaceutics*, *302*(1–2), 18–28.

Marques, H. M. C. (2010). A review on cyclodextrin encapsulation of essential oils and volatiles. *Flavour and Fragrance Journal*, *25*(5), 313–326.

Nieddu, M., Rassu, G., Boatto, G., Bosi, P., Trevisi, P., Giunchedi, P., et al. (2014). Improvement of thymol properties by complexation with cyclodextrins: In vitro and in vivo studies. *Carbohydrate Polymers*, *102*(1), 393–399.

Pinho, E., Grootveld, M., Soares, G., & Henriques, M. (2014). Cyclodextrins as encapsulation agents for plant bioactive compounds. *Carbohydrate Polymers*, *101*(1), 121–135.

Rao, V. M., & Stella, V. J. (2003). When can cyclodextrins be considered for solubilization purposes? *Journal of Pharmaceutical Sciences*, *92*(5), 927–932.

Seo, E. J., Min, S. G., & Choi, M. J. (2010). Release characteristics of freeze–dried eugenol encapsulated with β-cyclodextrin by molecular inclusion method. *Journal of Microencapsulation*, *27*(6), 496–505.

Shao, P., Zhang, J., Fang, Z., & Sun, P. (2014). Complexing of chlorogenic acid with β-cyclodextrins: Inclusion effects, antioxidative properties and potential application in grape juice. *Food Hydrocolloids*, *41*, 132–139.

Singh, R., Bharti, N., Madan, J., & Hiremath, S. N. (2010). Characterization of cyclodextrin inclusion complexes—A review. *Journal of Pharmaceutical Science and Technology*, *2*(3), 171–183.

Szejtli, J. (1998). Introduction and general overview of cyclodextrins chemistry. *Chemical Reviews*, *98*(5), 1743–1753.

Turek, C., & Stintzing, F. C. (2013). Stability of essential oils: A review. *Comprehensive Reviews in Food Science and Food Safety*, *12*(1), 40–53.

Vandelli, M. A., Ruozi, B., Forni, F., Mucci, A., Salvioli, G., & Galli, E. (2000). A solution and solid state study on 2-hydroxypropyl-β-cyclodextrin complexation with hyodeoxycholic acid. *Jounal of Inclusion Phenomena and Marcocyclic Chemistry*, *37*(1–4), 237–251.

Wang, X., Luo, Z., & Xiao, Z. (2014). Preparation, characterization, and thermal stability of β-cyclodextrin/soybean lecithin inclusion complex. *Carbohydrate Polymers*, *101*(1), 1027–1032.

Yang, Y., & Song, L. X. (2005). Study on the inclusion compounds of eugenol with α-, β-, γ- and heptakis (2,6-di-*O*-methyl)-β-cyclodextrins. *Journal of Inclusion Phenomena and Macrocyclic Chemistry*, *53*(1–2), 27–33.

Yuan, C., Lu, Z., & Jin, Z. (2014). Characterization of an inclusion complex of ethyl benzoate with hydroxypropyl-β-cyclodextrin. *Food Chemistry*, *152*(1), 140–145.

Zeller, A., Horst, K., & Rychlik, M. (2009). Study of the metabolism of estragole in humans consuming fennel tea. *Chemical Research in Toxicology*, *22*(12), 1929–1937.